



NONLINEAR TIME-HISTORY ANALYSIS OF A POWER BOILER SUPPORT STRUCTURE UNDER EARTHQUAKE LOADING

Ernesto Cruz¹, Rodrigo Garcia² and Dania Valdivia³

ABSTRACT

As part of a research effort in the general field of expected design performance and nonlinear behavior of heavy industrial structures, this study deals with the response of a power boiler support structure using nonlinear time-history analysis using ground motions that simulate the level of earthquake action considered for the design condition. Four actual structures with the same configuration as the one studied are presently being built in Chile; therefore the results of this study provide some relevant insight on the expected seismic behavior of them.

The dynamic response was calculated using an implementation of the Fast Nonlinear Analysis method (FNA) developed by E. Wilson considering as basis for the elastic solution a large set of the eigenvectors of the problem. Given that the structure is a concentrically braced frame, the model considers different types of nonlinear elements defining nonlinearity in braces, columns, pedestals, and in seismic stoppers, each one with its own force-deformation relation. The earthquake ground motion data used is a set of nine records of the March 1985 earthquake in central Chile. Each record is scaled to obtain the same value of the Housner Intensity parameter as that corresponding to the Acceleration Design Spectrum of the Chilean code for Seismic Design of buildings (considering 5% damping ratio and Seismic Zone 1 ($A_0 = 0.4g$), Intermediate Soil conditions).

The results obtained show that “seismic stoppers” and “anchor bolts” are the elements most susceptible to reach a high non-linear behavior demand for the level of earthquake intensity considered (Chilean Code, Life Safety level, $R=2.5$). Vertical plane bracings (in the direction of earthquake action) and horizontal bracings have also rather large demands but the demand on vertical bracings in planes perpendicular to the earthquake action direction and in columns is almost negligible. The drift values obtained between the main platforms levels was always smaller than the maximum drift allowed in the Chilean code. A rather good correlation was obtained between the values of the demand to capacity ratio of the different elements in the standard design procedure (based on reduced elastic response forces) and the element forces and deformation demand obtained in the nonlinear analysis.

¹Professor, Dept. of Structural Engineering, P. Universidad Católica de Chile, Santiago, Chile. ecruz@ing.puc.cl

²M.Sc., Research Assistant. Pontificia Universidad Católica de Chile, Santiago, Chile. ragarcin@uc.cl

³M.Sc., Principal, EQCO Earthquake Engineering Consultants, Santiago, Chile. danial@eqcoeng.com

Introduction

In the typical seismic design, the use of lateral forces or response spectrum on a simple linear structure is not able to answer the question “how will the structure really behave when a big earthquake comes?” The usual contracts for the design of heavy industrial structures do not usually allow enough time to use sophisticated verification methods, leaving the safety in the strict compliance with seismic design codes.

In this study, we carry out the real response of a power boiler support structure by nonlinear time history analysis, finding relations between the expected design and the observed response.

Boiler Model and Input Data

The boiler model includes the support steel structure modeled with standard “frame type” members and the mechanical components (internal parts) modeled as simplified finite elements or single lumped masses. The total seismic weight is 100,910 kN. The boiler was designed according with the current Chilean seismic code (INN 2003) and the AISC specifications (2005). Figure 1 shows the overall shape of the structure based on the rendering of the analysis model.

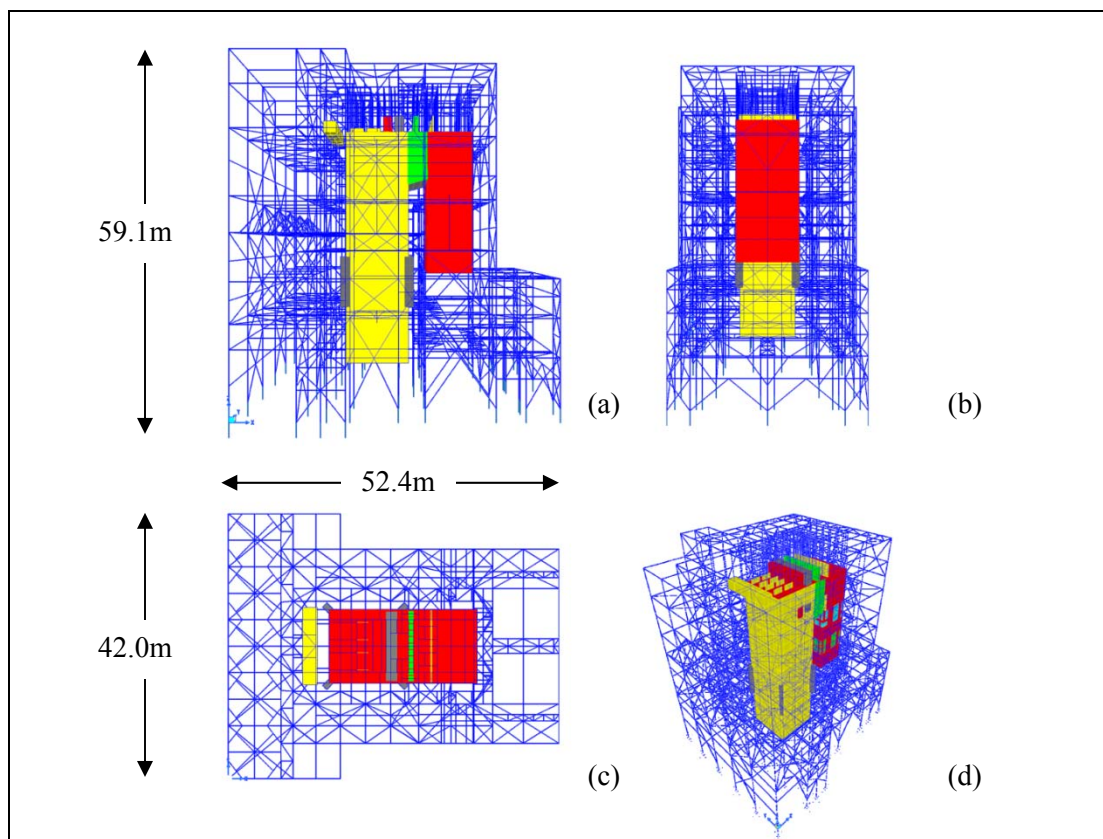


Figure 1. 3D views of boiler model; a) YZ view, b) XZ view, c) XY view (from top without perspective) and d) 3D general view.

For the time history analysis, nine acceleration records obtained from the Chilean earthquake of March 1985 were scaled to the same Housner intensity of the elastic response

spectrum of the NCh433of96 code for soil type 3 in seismic zone III (INN 1996). Note that this normalization of the records is independent of the structure properties, but it leads to similar values of base shear at those obtained from a response spectrum analysis for the different records. The earthquake action is considered acting in a single direction, in order to compare with the normal procedures used for the design of these types of structures.

The model considers nonlinear behavior in all elements in which the design was controlled by a seismic load combination. For all of them, the limit strength was calculated using the AISC 2005 code, without the safety factors and considering the effective yield stress ($R_y \cdot F_y$). The three types of nonlinearity implemented in this study are described next.

Bracings

The force-deformation relations used to model these uniaxial elements consider an approximation of nonlinear effects produced by plastification of the material and buckling (see Figure 2). The shape of the curve was calibrated for non-slender sections according to the seismic code design provisions that require using compact sections and a maximum “demand to capacity ratio” on the design of 0.8.

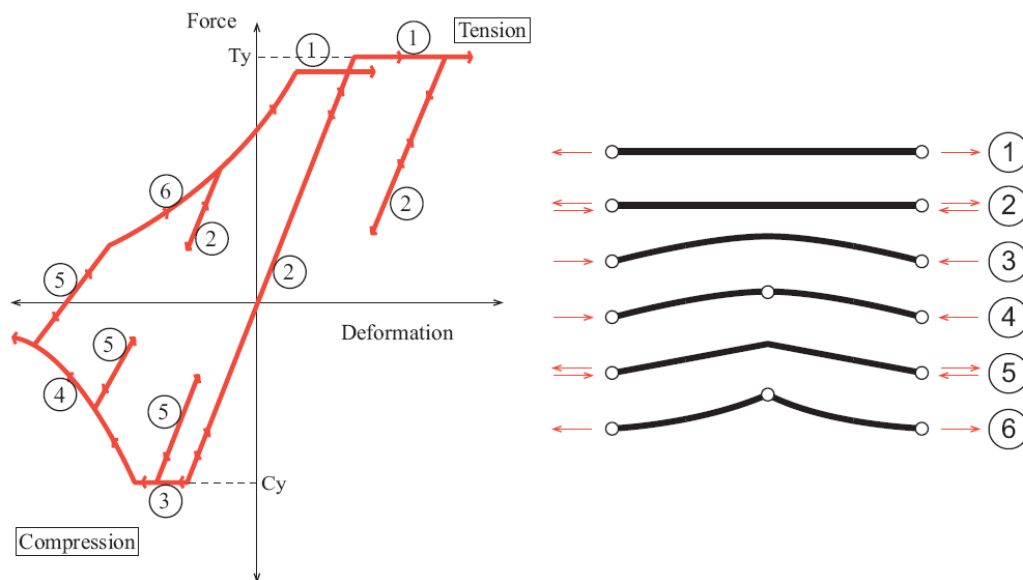


Figure 2. Force-deformation curve for bracings: (1) Yield plateau in tension, (2) Elastic zone, (3) Buckling plateau, (4) Buckling zone with second order effects, (5) Elastic zone with second order effects and (6) Inelastic unload zone with second order effects.

Columns and Stoppers

The columns are the main system to distribute the gravity loads to the foundation and the skeleton of the structure. The stoppers have the function to restrain the relative lateral displacement between the internal hanging parts of the boiler and the support structure to a very small gap in several levels over the height (see Figure 3).

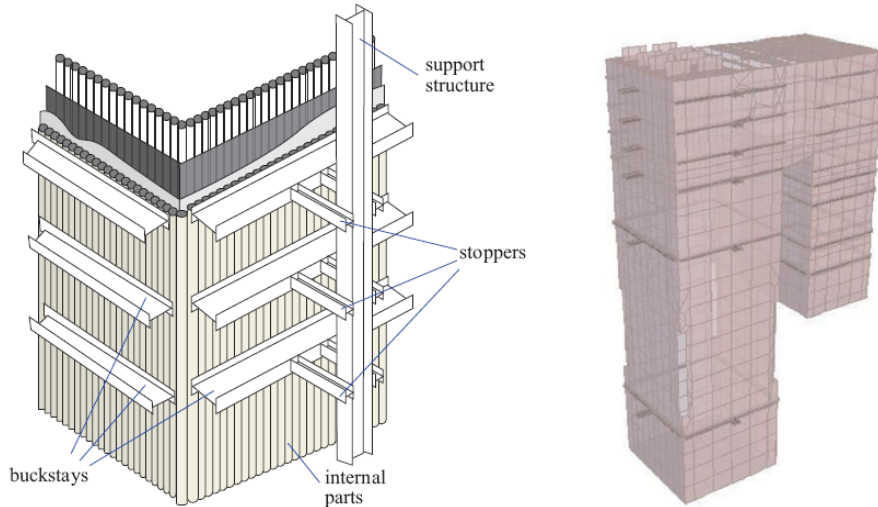


Figure 3. Schematic representation of stoppers, a) Representation of stopper system, b) View of internal parts, buckstays, and stoppers in the computational model.

For these elements, a lumped-plasticity model at each element end is considered, taking into account the 3D interaction between the axial load and the bending moments (in the strong and weak axis) of the section. A “smooth” yield surface was used, based in the AISC 1989 equations, according to the recommendation by McGuire (2000). When increments of deformation produce restoring force combinations that fall outside of the yield surface, the stiffness associated to the tangent plane of the surface can be estimated. Using this approach in numerical integration, the use of tangent planes to the convex surfaces will always provide force combinations that lay outside of the surface and it is necessary to correct the results. A central correction scheme was used. The procedure preserves the axial load value, but tries to bring the moment values to the center up to touching the yield surface.

Pedestals

The nonlinearity of this kind of elements is modeled according to the different actions over the concrete pedestal and anchor bolts, as shown in Figure 4.

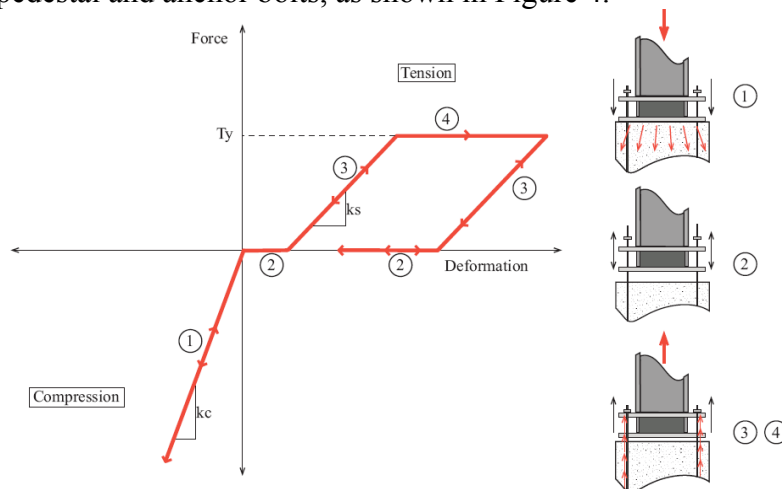


Figure 4. Force-deformation curve for pedestals: (1) Compression on concrete, (2) Non restrained zone, (3) Elastic tension of bolts and (4) Plastic tension of bolts.

The integration was carried out with a fourth-order Runge–Kutta method with a time step of 0.0025 seconds. To solve the nonlinear equations of movement, a Fast Nonlinear Analysis method (FNA, Wilson, 2003) with 700 modes was used (total number of mass degrees of freedom is 15,093). This method uses modal decomposition to reduce the number of degrees of freedom of the structure, but keeps the coupling between the modal coordinates in the nonlinear forces interacting over them. The equation of motion for this method is:

$$\phi^T \mathbf{M} \phi \ddot{\mathbf{q}} + \phi^T \mathbf{C} \phi \dot{\mathbf{q}} + \phi^T \mathbf{K} \phi \mathbf{q} = \phi^T \mathbf{F}_{NL}(\phi \dot{\mathbf{q}}, \phi \mathbf{q}, t) - \phi^T \mathbf{M} \mathbf{r} \ddot{u}_g(t) \quad (1)$$

where \mathbf{M} , \mathbf{C} and \mathbf{K} are the mass, damping and stiffness matrices respectively, ϕ is a matrix with the mode shapes considered, \mathbf{F}_{NL} is the nonlinear forces vector, \mathbf{r} the seismic incidence vector and, \ddot{u}_g is the ground acceleration (the input, only considered in one direction to properly normalize it).

The selected modes were obtained solving the standard eigenvalue problem and not by the special load-dependent Ritz vectors algorithm normally used for the FNA method. The number of modes used is not enough for problems with large amount of nonlinearity, but it is accurate for problems with the levels of nonlinearity observed in this study (García, 2009)

A rigorous application of the FNA method would imply the use of more than 4,500 modes, with the lowest period near $2e-6$ seconds. This situation forces the use of very large fully populated matrices and very small integration time steps that increase the computational cost nearly 25,000 times. Table 1 shows the natural periods for the modes with larger participating mass ratios.

Table 1. List of main modes of the model.

Mode Number	Description	Period (s)	Participating mass ratios			
			Ux	Uy	Uz	Rz
1	Steam drum (Y translation)	20.035	-	3.1%	-	-
17	Steam drum (X translation)	1.925	7.6%	-	-	3.2%
27	Global bending in X dir.	1.274	28.0%	-	0.3%	10.3%
28	Global bending in X dir.	1.236	10.7%	0.1%	0.6%	3.1%
37	Internal parts mode (Y dir.)	1.187	0.6%	4.1%	-	3.0%
41	Global bending in X dir.	1.157	13.5%	-	1.6%	5.6%
47	Global bending in Y dir.	1.045	-	28.4%	-	14.7%
50	Global bending in Y dir.	1.007	-	34.3%	-	11.4%
416	Coal silos vertical transl.	0.255	-	-	31.6%	-
700	Last mode used	0.146	-	-	-	-
TOTAL			98.0%	97.3%	72.0%	96.7%

Global Seismic Performance

The global performance can be observed in terms of three main response quantities: base

reactions (base shears), roof displacement, and drift between platform levels at different heights. The base reaction gives an idea of total strength of the structure, the roof displacement of its level of deformation, and the drifts a notion of the expected damage level. Average values over the set of nine records are shown for the results.

As seen in Table 2, in the X direction (longitudinal), the maximum horizontal base reactions observed shows values very similar to linear response. In the Y direction (transversal), the maximum values have an average reduction of 9%. This could be explained by the smaller strength of the XZ resistant planes that produces, for the same earthquake record, more inelastic demand over the elements, requiring more energy dissipation and less base reaction values. In both cases, the “nonlinear” case values are similar to the linear case values.

Table 2. Maximum horizontal base reactions and roof lateral displacements. The values shown have the same direction of the earthquake action.

Average Values	Earthquake X				Earthquake Y			
	Linear	Nonlinear +X	Nonlinear -X	Average L/NL	Linear	Nonlinear +X	Nonlinear -X	Average L/NL
Base Reaction [kN]	49031	48855	48622	1.01	68582	62038	62082	1.10
Roof Displ. [cm]	33.6	31.6	31.7	1.06	41.3	35.0	35.0	1.16

To measure the roof displacements, a well braced node of the roof was selected. Note that no rigid diaphragm exists on the roof and the displacement values at other nodes can be different.

Regarding the horizontal displacements of the roof shown in Table 2; note that for both directions, the values from the linear case are larger than the values for the nonlinear case; in spite of the fact that nonlinear behavior should make the structure “less stiff.” This could be explained considering that the structure dissipates more energy when it has plastic deformations and the smaller stiffness of it does not necessarily imply larger displacements when the predominant vibration modes of the structure have long periods.

The time history curves of base reactions vs. roof displacement cannot be represented by a single degrees of freedom “constitutive” relation, even in the linear cases. The main reason for this is the large influence of two or more modes in the dynamic response, hindering any effort to associate the behavior with a single degree of freedom relation. This situation becomes even worse with nonlinear behavior.

In Figure 5 the maximum values of drift between platform levels for the boiler support structure are shown. The figure shows that nonlinear analyses results do not exceed the Chilean seismic code limit of 15%. The maximum drift occurs in a region where the structure has a large discontinuity of stiffness and the internal parts transfer most of the “seismic lateral forces” to the structure through the stoppers.

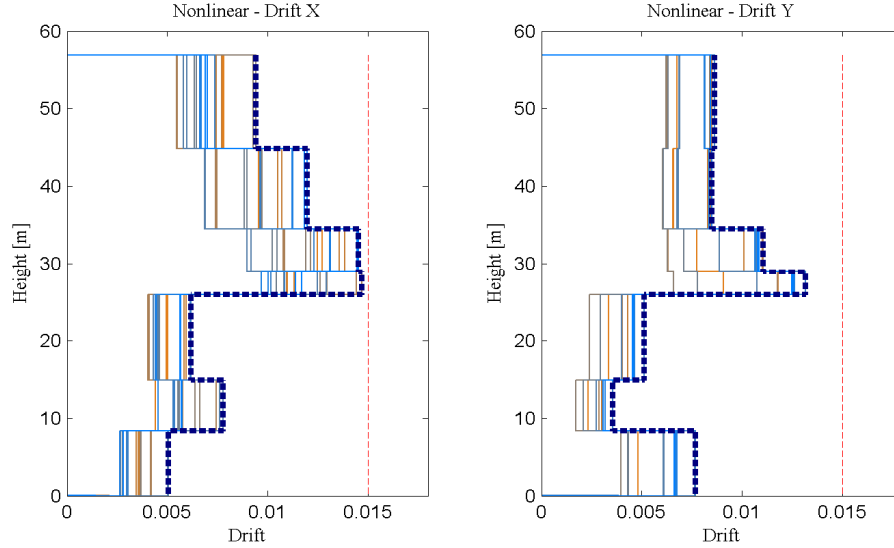


Figure 5. Drift between platform levels over the height for all the records and nonlinear analysis. The dark line is the envelope for all the analyzed cases. The direction for each drift shown is the same direction of the earthquake action.

Local Results

For this study, it is defined that an element is in the nonlinear range at a time t if at any time before t , the element has reached a nonlinear state, regardless of the amount of inelastic deformation involved.

For the level of intensity of earthquake ground motion used in this study, the typical sequence of nonlinear behavior demand is in first place the stoppers and pedestals, followed by the lateral bracing system in the same direction of the earthquake and the horizontal bracings and finally, an almost negligible demand in columns and in the lateral bracing system perpendicular to the earthquake action direction. Figure 6 shows an example of this sequence and Table 3 shows the average percentage of elements in the nonlinear range for all analyzed cases.

The individual performance for bracing elements shows hysteresis curves with little dissipation of energy. The nonlinear behavior for bracing elements usually starts in compression and it remains in the buckling plateau zone, without notorious second order effects.

Table 3. Number of elements in nonlinear range at the end of each earthquake record.

Nonlinear element type	Short name	Number of elements	Earthquake X		Earthquake Y	
			\bar{X}	σ_x	\bar{X}	σ_x
Bracings (YZ plane)	BRCX	244	0%	0%	41%	13%
Bracings (XZ plane)	BRCY	209	43%	9%	2%	1%
Bracings (Horizontal)	BRCZ	322	26%	5%	21%	7%
Pedestals	PED	54	74%	5%	66%	3%
Columns	CLM	695	1%	1%	3%	2%
Stoppers	STP	38	36%	7%	29%	3%

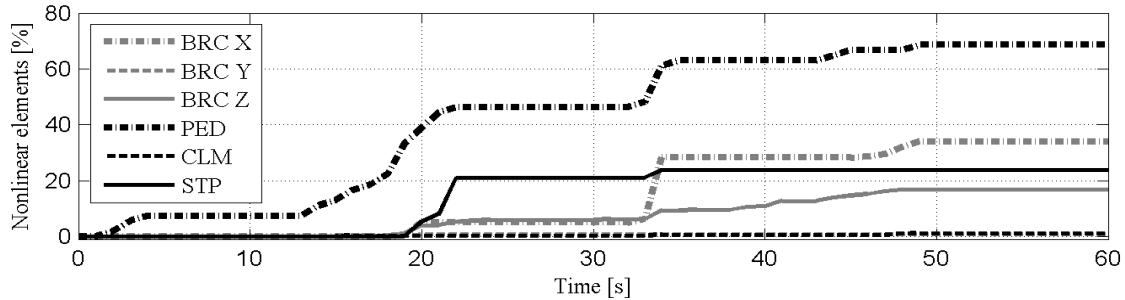


Figure 6. Percentage of elements in nonlinear range vs. time (seconds) for Llolleo 010 record in +Y direction. The nomenclature of elements is according Table 3.

The nonlinear performance of the bracings relative to the resisting planes they belong to is shown as example only for XZ planes in Table 4. The demand on the bracing planes transversal to earthquake direction is only observed in few cases on the YZ planes located at the ends of the structure for the earthquakes in +Y direction and it could be explained due to the significant torsional effects when the earthquake acts in this direction. The horizontal bracing systems have a uniform distribution with larger nonlinear demand caused by a local distribution of forces from the most demanded stoppers of the structure.

To compare the design with the performance of the bracing elements, an element level ductility ratio μ is defined as the ratio between the difference of all values and the sum of the yield deformations in both directions considering ideal elasto-plastic behavior.

Figure 7 shows the relation between the number of elements in the nonlinear range and “demand to capacity ratio” on the design. Figure 8 shows the relation between the element ductility ratio and “demand to capacity ratio” on the design for the XZ planes. Note that the demand to capacity ratio is always less than 80% according to the Chilean seismic code requirements for bracings. The results show a good correlation between the demand to capacity ratio of bracings on the design and the level of ductility observed and the amount of nonlinear elements.

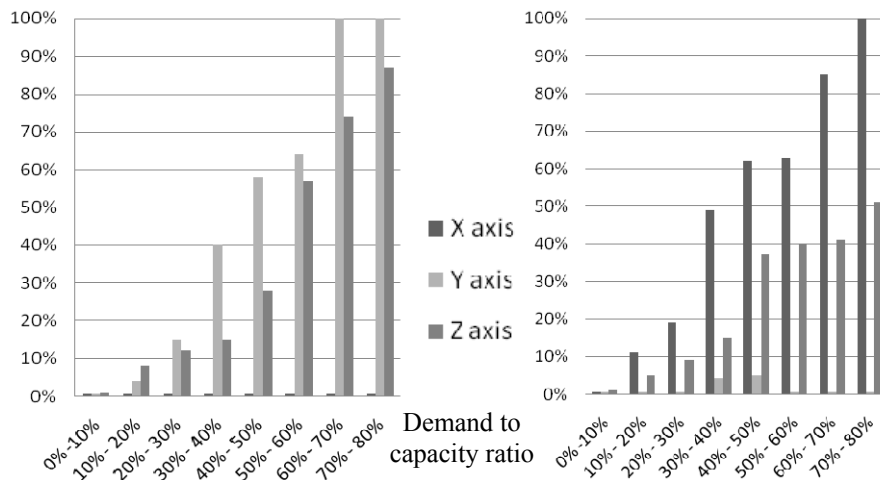


Figure 7. Number of bracings in nonlinear range for different demand to capacity ratio ranges, a) Earthquake X, b) Earthquake Y.

Table 4. Number of lateral bracings in nonlinear range for XZ planes.

XZ plane location [cm]	Number of elements	Earthquake X		Earthquake Y	
		\bar{X}	σ_x	\bar{X}	σ_x
Y= 0	26	41%	15%	7%	3%
Y= 560	36	52%	8%	2%	2%
Y= 1185	28	59%	10%	0%	-
Y= 2100	13	12%	15%	0%	-
Y= 3015	28	54%	8%	0%	-
Y= 3640	36	47%	10%	2%	2%
Y= 4200	26	30%	15%	3%	1%

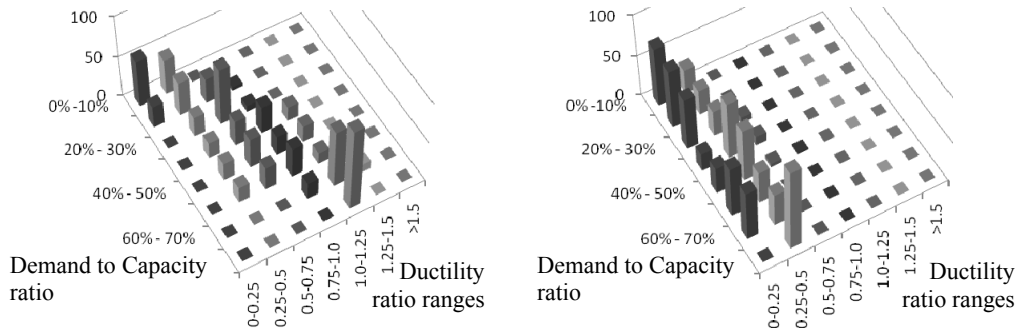


Figure 8. Distribution of ductility values for lateral bracings in XZ plane vs. demand to capacity ratio, a) Earthquake X, b) Earthquake Y.

On the other hand, the results for stoppers show that these elements have a large demand. In the response curves, null participation of axial forces and the multiple plastic cycles are seen. These elements are shown to be an important source of energy dissipation in the response.

Table 5. Number of stoppers in nonlinear range of behavior.

XY planes location [cm]	Number of elements	Earthquake X		Earthquake Y	
		\bar{X}	σ_x	\bar{X}	σ_x
Z= 1310	4	44%	16%	50%	0%
Z= 2670	4	50%	0%	65%	13%
Z= 2950	4	50%	0%	64%	13%
Z= 3206	4	50%	0%	1%	6%
Z= 3406	4	25%	0%	50%	0%
Z= 3606	4	31%	20%	0%	-
Z= 3856	3	56%	23%	0%	-
Z= 4106	4	0%	-	0%	-
Z= 4366	4	11%	21%	17%	12%

Table 5 shows the number of stoppers in the nonlinear range. Note that each stopper level has 4 or 3 elements: 2 elements to resist loads in the X direction and 1 or 2 to resist loads in the Y direction. For this reason, the stoppers usually reach the nonlinear range in pairs and the average percentage values greater than 50% for some levels for earthquake in Y direction imply cases where the transverse direction stoppers system also “yields” for some seismic records.

Relative to pedestals, although these elements show an important number of elements in nonlinear range, in no case they reach plastic behavior, limiting the nonlinear behavior to the elastic tension of the anchor bolts, opposite to the expected results. The residual deformation of anchor bolts is one of the typical observations of damage after an earthquake of large intensity. This difference could be explained by the use of an ideal elasto-plastic model, ignoring the residual tensions on the bolts that may induce an earlier incursion in the nonlinear range.

Conclusions

The design provisions used in the analyzed structure was reflected in a seismic behavior very similar to an expected good performance. The most critical nonlinear behavior was concentrated in elements easy to repair (stoppers and anchor bolts), the columns had almost negligible nonlinear behavior and the demand over the lateral bracings was directly related with the “demand to capacity ratio” of the design of them. Furthermore, it can be concluded that the lateral resisting planes with more bracing elements have a larger percentage of elements in the nonlinear range and the most demanded horizontal bracing elements were directly related with the larger demands on stoppers that transfer large horizontal loads to the platforms.

In other hand, no relationship associated with a single degree of freedom system was found for this structure. This conclusion implies that the complex behavior of the boiler support could be bad represented in a capacity curve or a pushover analysis.

References

- AISC, 2005, *Specification for structural steel buildings*, American Institute of Steel Construction, Chicago, USA, 460 pp.
- García, R., 2009, Análisis Sísmico no lineal de la estructura de soporte de una caldera de potencia usando FNA. M.Sc. Thesis. Pontificia Universidad Católica de Chile, 2009.
- Instituto Nacional de Normalización (1996). Diseño Sísmico de Edificios. Norma NCh 433 Of. 1996. Santiago, Chile.
- Instituto Nacional de Normalización (2003). Diseño Sísmico de Estructuras e Instalaciones Industriales. Norma NCh 2369 Of. 2003. Santiago, Chile.
- McGuire, W., Gallagher, R. and Ziemian, R., 2000. *Matrix Structural Analysis*, 2nd edition, John Wiley & Sons, New York, NY, 460 pp.
- Wilson E., 2002, *Three-Dimensional Static and Dynamic Analysis of Structures*, 3rd Edition, Computer & Structures, Berkeley, CA, 398 pp.